BMC Medical Genomics

RESEARCH

Open Access

Pathogenomics of multidrug-resistant *Escherichia coli* from bloodstream infections in South Africa

Bakoena Ashton Hetsa[1], Esther Eyram Asare Yeboah[1,2], Arshad Ismail[3], Sabiha Yusuf Essack[1,4*] and Daniel Gyamfi Amoako[1*]

Abstract

Background *Escherichia coli* (*E. coli*) is a leading cause of bloodstream infections (BSIs) globally, with multidrug-resistant (MDR) strains complicating treatment outcomes. In South Africa, genomic data on such isolates remain scarce. To elucidate the genomic landscape of *E. coli* isolates from bloodstream infections (BSIs) collected over a one-year period in the uMgungundlovu District, South Africa, with a focus on the resistance and virulence genes, mobile genetic elements (MGEs), genetic synteny, sequence types (STs), and phylogenomic context.

Methods Twenty-five non-duplicate *E. coli* isolates were recovered from blood cultures and subjected to antimicrobial susceptibility testing. All twelve MDR isolates underwent whole-genome sequencing and bioinformatic analysis.

Results The MDR isolates comprised six distinct STs, notably high-risk international lineages ST131 (33.3%) and ST69 (25.0%), spanning five phylogroups, predominantly B2 and D. Eight O: H serotypes were identified, with O25:H4 and O45:H16 being most frequent. CH-typing revealed dominant CH types CH40-30 (ST131) and CH35-27 (ST69) and *fimH* alleles such as *fimH30* and *fimH27*. The isolates encoded β-lactamases, including $bla_{\text{CTX-M-15}}$, $bla_{\text{TEM-1B}}$ and $bla_{\text{OXA-1,}}$ frequently co-located with MGEs. Notably, $bla_{\text{CTX-M-15}}$ was chromosomally integrated within a Tn*3*–IS*Ecp1* transposon unit, while $bla_{\text{TEM-1B}}$ and $bla_{\text{OXA-1}}$ were associated with diverse plasmid-associated syntenic architectures flanked by IS*1*, IS*91*, or integron-associated regions. Other antibiotic resistance genes were detected, conferring resistance to aminoglycosides (*aph(3')-Ia*, *aac(3)-IIa*, *aac(3)-IIe*, *aadA1*, *aadA2*), sulfonamides (*sul1*, *sul2*) and trimethoprim (*dfrA* variants). A diverse array of virulence genes was identified, associated with adhesion, iron acquisition, serum resistance, and toxin production. Phylogenomic clustering revealed close relationships between local ST131/ST69 isolates and counterparts across Africa.

Conclusions The study identifies diverse MDR *E. coli* clones circulating in bloodstream infections, notably high-risk lineages ST131, ST69 and ST10, with complex resistance and virulence gene arsenals facilitated by MGEs. These

*Correspondence:
Sabiha Yusuf Essack
essacks@ukzn.ac.za
Daniel Gyamfi Amoako
amoakodg@gmail.com

Full list of author information is available at the end of the article

insights reinforce the imperative for genomic surveillance to guide infection control and antibiotic stewardship in high-burden settings.

Keywords *Escherichia coli*, Bloodstream infection, Pathogenomics, Multidrug resistance, High-risk clones, Molecular typing, Phylogenetics, South Africa

Background

Escherichia coli (*E. coli*) is among the leading causes of bloodstream infections (BSIs) worldwide, with surveillance programmes such as WHO GLASS and EARS-Net consistently reporting its prominence across diverse healthcare settings [1–3]. Global burden assessments further rank *E. coli* among the top pathogens associated with antimicrobial resistance (AMR)–related mortality [4]. In sub-Saharan Africa, recent studies highlight concerning rates of AMR among invasive *E. coli* isolates, underscoring the need for enhanced genomic surveillance across the region [5].

The treatment of *E. coli*-associated BSIs is increasingly challenged by the emergence and dissemination of AMR, especially multidrug resistance (MDR). Globally, *E. coli* has demonstrated escalating resistance to commonly used antibiotics including β-lactams, aminoglycosides, tetracyclines, and fluoroquinolones [6–8]. Of particular concern is the widespread presence of extended-spectrum β-lactamases (ESBLs) such as $bla_{\text{CTX-M-15}}$, which confer resistance to third-generation cephalosporins, key agents in the empirical management of sepsis [6, 9–11]. Furthermore, mobile genetic elements (MGEs), such as insertion sequences, transposons, and integrons, play a key role in facilitating horizontal gene transfer and accelerating the spread of resistance traits both within and between bacterial species [12, 13].

Recent whole-genome sequencing (WGS) studies have revealed that *E. coli* populations responsible for BSIs are not only genetically diverse but also geographically structured, with specific sequence types (STs) such as ST131, ST69, ST10, and ST38 recurrently identified across continents [14–16]. These high-risk lineages; ST131/phylogroup B2, ST69/phylogroup D, and ST10/phylogroup A, commonly harbor complex resistance and virulence-associated genes, facilitating their persistence across both community and healthcare settings [14, 17, 18]. Despite this growing body of knowledge, genomic data on *E. coli* strains implicated in BSIs in sub-Saharan Africa remain sparse, limiting our understanding of their epidemiology and evolutionary dynamics in high-burden, resource-limited settings [19, 20].

In South Africa, fragmented surveillance systems and limited access to molecular diagnostics have hindered comprehensive assessments of bloodstream pathogens and their resistance mechanisms [20]. As a result, there is a critical gap in local genomic surveillance data needed to guide antimicrobial stewardship and infection prevention strategies. This study aimed to characterize the genomic features of *E. coli* isolates recovered from BSIs in patients admitted to public hospitals in the uMgungundlovu District, South Africa. Using WGS, we explored the isolates' AMR profiles, virulence gene content, sequence types, phylogenetic structure, and associated MGEs.

Methods

Bacterial collection and identification

A total of 25 non-duplicate *E. coli* isolates were recovered from blood cultures collected between November 2017 and December 2018 at two public hospitals in the uMgungundlovu District, KwaZulu-Natal Province, South Africa. These isolates comprised all eligible *E. coli* BSIs identified in the two facilities during the study period. Species identification was performed using the VITEK® 2 automated system (BioMérieux, Marcy-l'Étoile, France) in accordance with the manufacturer's guidelines.

Phenotypic antimicrobial susceptibility testing and MDR isolates

Antimicrobial susceptibility testing was performed using the Kirby-Bauer disk diffusion method. Results were interpreted according to the European Committee on Antimicrobial Susceptibility Testing [21] guidelines; where EUCAST breakpoints were unavailable, Clinical and Laboratory Standards Institute (CLSI, 2020) criteria were applied. A total of 20 antibiotics were tested, including: amikacin (AMK, 30 µg), ampicillin (AMP, 10 µg), amoxicillin-clavulanic acid (AMC, 30 µg), azithromycin (AZM, 15 µg), cefepime (FEP, 10 µg), cefotaxime (CTX, 30 µg), cefoxitin (FOX, 30 µg), ceftazidime (CAZ, 30 µg), ceftriaxone (CRO, 30 µg), cephalexin (LEX, 30 µg), ciprofloxacin (CIP, 5 µg), chloramphenicol (CHL, 30 µg), gentamicin (GEN, 10 µg), imipenem (IPM, 10 µg), meropenem (MEM, 10 µg), nalidixic acid (NAL, 30 µg), piperacillin-tazobactam (TZP, 110 µg), tetracycline (TET, 30 µg), tigecycline (TGC, 15 µg), and trimethoprim-sulfamethoxazole (SXT, 25 µg). All antibiotic discs were sourced from Oxoid Ltd. (Basingstoke, UK) (Table S1). *E. coli* ATCC 25,922 served as the quality control reference strain. MDR was defined as resistance to at least one agent in three or more antimicrobial classes, in accordance with international consensus criteria [22]. Isolates exhibiting MDR phenotypes were selected for WGS.

DNA extraction and sequencing

Genomic DNA was extracted from MDR *E. coli* isolates using the GenElute™ Bacterial Genomic DNA Kit (Sigma-Aldrich, St. Louis, MO, USA), following the manufacturer's instructions. DNA quality and purity were assessed using a NanoDrop™ 8000 spectrophotometer (Thermo Scientific, Waltham, MA, USA). Sequencing libraries were prepared using the Nextera XT DNA Library Preparation Kit (Illumina, San Diego, CA, USA) and sequenced on the Illumina NextSeq platform (Illumina, San Diego, CA, USA). Raw sequencing reads were quality-trimmed using Sickle v1.33 (https://github.com/najoshi/sickle), and de novo assembly was performed using SPAdes v3.6.2 (https://cab.spbu.ru/software/spades/). Assembled genomes were submitted to GenBank under BioProject accession number PRJNA669537.

Genomic analysis and annotation

Multilocus sequence typing (MLST), serotyping (O and H antigens), and *fimH* typing were performed using tools hosted by the Center for Genomic Epidemiology (CGE): MLST 2.0 (https://cge.cbs.dtu.dk/services/MLST/, accessed 10 April 2025), SerotypeFinder 2.0 (https://cge.food.dtu.dk/services/SerotypeFinder/, accessed 10 April 2025), and FimTyper 1.0 (https://cge.food.dtu.dk/services/FimTyper/, accessed 12 April 2025).

Antibiotic resistance genes (ARGs) were identified using ResFinder v4.6 (≥ 60% coverage, ≥ 90% identity) (https://genomicepidemiology.org/services/ResFinder/, accessed 15 April 2025) and the Resistance Gene Identifier (RGI) tool from the Comprehensive Antibiotic Resistance Database (CARD) (default parameters: strict and perfect matches) (https://card.mcmaster.ca/analyze/rgi, accessed 15 April 2025). Virulence factors were detected using VirulenceFinder 2.0 (https://cge.food.dtu.dk/services/VirulenceFinder/, accessed 16 April 2025) (≥ 60% coverage, ≥ 90% identity).

Mobile genetic elements were identified using MobileElementFinder (https://cge.food.dtu.dk/services/MobileElementFinder/, accessed 26 April 2025), ISFinder (https://www-is.biotoul.fr/, accessed 26 April 2025), PlasmidFinder 1.3 (https://cge.cbs.dtu.dk/services/PlasmidFinder/, accessed 16 April 2025) and the INTEGRALL database (http://integrall.bio.ua.pt/, accessed 26 April 2025). MobileElementFinder results were interpreted using default thresholds (≥ 90% identity and ≥ 60% coverage). ISFinder matches were assigned exact insertion sequence (IS) names only when the identity was ≥ 95%; hits with 80–95% identity were classified as related IS variants rather than the canonical element. Integron-associated genes identified through INTEGRALL were assigned only when ≥ 95% identity and ≥ 90% coverage were met. Elements detected below these thresholds are described as "related variants" or "IS-like elements" to avoid implying exact equivalence with reference MGEs. The synteny and genetic environment of ARGs and associated MGEs were examined using annotated GenBank files. Comparative multi-isolate loci were visualized with clinker v0.0.32 (https://github.com/gamcil/clinker, accessed 15 March 2026), whereas single-isolate regions were presented as linear functional maps using the same colour scheme for consistency. ARGs were classified as plasmid-associated when detected on the same contig as a plasmid replicon; however, definitive plasmid structures and architectures could not be resolved using short-read sequencing data alone.

Phylogenomics and epidemiological insights

Phylogenomic analysis was performed to assess the genetic relatedness of the study isolates to other *E. coli* strains from South Africa and the broader African continent, with a specific focus on isolates recovered from blood samples. Publicly available genomes were retrieved from the Bacterial and Viral Bioinformatics Resource Center (BV-BRC) database (https://www.bv-brc.org/, accessed 25 May 2025), annotated, and integrated into the comparative analysis. A core genome phylogenetic tree was constructed using the BV-BRC Phylogenetic Tree Building tool, which aligns nucleotide and amino acid sequences from 1000 conserved genes to infer evolutionary relationships. *E. coli fergusonii strain 40 A* was included as an outgroup reference strain to root the phylogenetic tree. The resulting tree was visualized using the Interactive Tree of Life (iTOL) platform (https://itol.embl.de/, accessed 25 May2024), where isolate-specific metadata including country of origin, year of isolation, and MLST were incorporated as color-coded outer rings to facilitate intuitive interpretation of the phylogenetic structure.

Results

Demographic details

The majority of isolates were recovered from a regional hospital ($n = 9$; 75%), while the remaining three originated from a tertiary care facility ($n = 3$; 25%). Isolates were collected from a variety of clinical wards, most frequently from the intensive care unit (ICU) and surgical ward ($n = 2$ each; 16.7%). The remaining isolates were each recovered from the casualty department, paediatric ward, outpatient orthopaedic clinic, emergency department, medical ward, surgical intensive care unit, and renal unit ($n = 1$ each). The gender distribution was balanced, with six isolates obtained from male patients and six from females (Table S1).

Phenotypic antibiotic susceptibility profiles of isolates

All the isolates exhibited phenotypic resistance to multiple β-lactam antibiotics, including penicillins (ampicillin,

β-lactam/β-lactamase inhibitor combinations (amoxicillin-clavulanate and piperacillin-tazobactam), cephamycins (cefoxitin, and extended-spectrum cephalosporins (cefotaxime, ceftazidime, ceftriaxone, and cefepime). Resistance to aminoglycosides (gentamicin and amikacin) and the ciprofloxacin was also observed (Fig. 1). Despite widespread multidrug resistance (MDR), most isolates remained susceptible to tigecycline, imipenem, and meropenem, with each exhibiting a low resistance rate of 8.3%. In contrast, resistance to chloramphenicol was observed in 25% of the isolates. All isolates were classified as MDR, defined as resistance to at least one agent in three or more antimicrobial classes. The observed phenotypic resistance patterns were supported by genotypic data obtained through WGS, which identified corresponding ARGs (Table 1).

Genome characteristics

The genomic features of the *E. coli* isolates, including genome size, sequencing coverage, L50, N50, GC content, number of RNA elements, and coding sequences, are summarized in Table S2. The total assembled genome sizes ranged from 4.8 to 6.1 Mb, with GC content values between 50.3% and 50.8%.

MLST analysis, serotype, phylogroup, CH-types and fimH type

A diverse distribution of sequence types, serotypes, phylogroups, CH-types, and *fimH* alleles was observed among the MDR *E. coli* isolates. MLST revealed six distinct STs, ST131 being the most prevalent ($n=4$, 33.3%), followed by ST69 ($n=3$, 25.0%) and ST10 ($n=2$, 16.7%) (Table 1). The isolates exhibited eight different O: H serotypes, the most frequent being O25:H4 ($n=3$, 25.0%) and O45:H16 ($n=2$, 16.7%) (Table 1). Other serotypes included O169:H4, O22:H4, O86:H18, O17:H18, O1:H7, and O30:H25, each represented by a single isolate. One isolate (E18) was non-typable for the O antigen but was assigned H4 (Fig. 2).

Phylogroup analysis assigned the isolates to five phylogroups: B2 ($n=4$, 33.3%), D ($n=4$, 33.3%), A ($n=2$, 16.7%), B1 ($n=1$, 8.3%), and F ($n=1$, 8.3%). Notably, a strong association between ST and phylogroup was observed. All ST131 isolates belonged to phylogroup B2, while all ST69 isolates clustered within phylogroup D. The two ST10 isolates were assigned to phylogroup A, while ST155 and ST59 belonged to phylogroups B1 and F, respectively (Fig. 2).

CH typing revealed eight distinct CH-types. The most frequent were CH40-30 ($n=3$, 37.5%) and CH35-27 ($n=3$, 37.5%), corresponding to ST131 and ST69 isolates, respectively (Table 1). Analysis of *fimH* alleles revealed a high degree of diversity, with *fimH27* being the most common ($n=4$, 40.0%), primarily associated with ST69 ($n=3$) and one ST10 isolate. Three ST131 isolates carried the *fimH30* allele, whereas one ST131 isolate (E26) harbored *fimH22*. Overall, isolates with the same ST and phylogroup shared the same *fimH* type, with the exception of E26, which diverged by *fimH* allele (Fig. 2).

Resistance gene analysis

A total of 31 distinct ARGs were identified (Table 1). All the isolates harbored β-lactamases; $bla_{\text{TEM-1B}}$ ($n=6$), $bla_{\text{OXA-1}}$ ($n=2$), $bla_{\text{CTX-M-15}}$ ($n=1$). Genes conferring

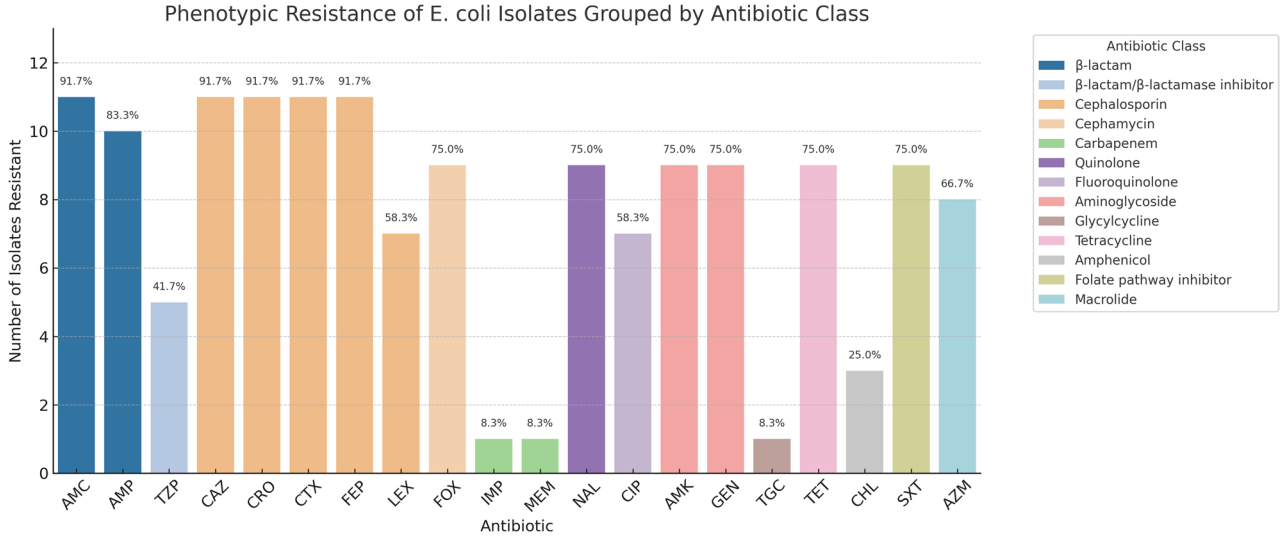

Fig. 1 The bar plot displays the number and percentage of resistant isolates per antibiotic, grouped by antimicrobial class. *AMP* Ampicillin, *AMC* Amoxicillin-clavulanic acid, *TZP* Piperacillin-tazobactam, *CTX* Cefotaxime, *CAZ* Ceftazidime, *CRO* Ceftriaxone, *FEP* Cefepime, *LEX* Cephalexin, *FOX* Cefoxitin, *IMP* Imipenem, *MEM* Meropenem, *NAL* Nalidixic acid, *CIP* Ciprofloxacin, *AMK* Amikacin, *GEN* Gentamicin, *TGC* Tigecycline, *TET* Tetracycline, *CHL* Chloramphenicol, *SXT* Trimethoprim-sulfamethoxazole, *AZM* Azithromycin

Table 1 Genomic features and antibiotic resistance genes of *E. coli* isolates from bloodstream infections

Isolate ID	Molecular typing					Antibiotic resistance genes		
	MLST	Serotype	Phylo type	Fimtype	CH-Type	β-lactamases	Aminoglycoside-modifying enzymes	Other ARGs
E3	ST131	O22:H4	B2	*fimH30*	CH40-30	bla_{TEM-1B},bla_{EC}	*aac(3)-IIa*, *aph(3')-Ia*, *aadA5*, *aac(3)-IIe*	*sul1*, *dfrA17*, *mph(A)*
E4	ST131	O25:H4	B2	*fimH30*	CH40-30	bla_{OXA-1}, $bla_{CTX-M-15}$, bla_{TEM-1B},bla_{EC}	*aac(6')-Ib-cr*, *aph(3")-Ib*, *aph(6)-Id*	*tet(B)*, *catB*, *sul2*, *dfrA14*, *mph(A)*, *mrx*, *tet(R)*
E26	ST131	O25:H4	B2	*fimH22*	CH40-30	bla_{TEM-1B},bla_{EC}	*aph(3")-Ib*, *aph(6)-Id*	*sul2*
S18	ST131	O25:H4	B2	*fimH30*	CH40-30	bla_{TEM-1B},bla_{EC}	*aph(6)-Id*, *aph(3")-Ib*, *aadA5*	*tet(A)*, *sul1*, *sul2*, *qacE*, *dfrA17*, *mph(A)*
E18	ST10	O^{NT}:H4	A	*fimH27*	CH11-27	bla_{TEM-1B}	*aph(6)-Id*	*tet(A)*, *sul2*, *sul1*, *dfrA14*, *dfrA7*, *qacE*, *mdf(A)*
S7	ST10	O169:H4	A	*fimH215*	CH11-1553	-	*aph(6)-Id*, *aph(3")-Ib*	*tet(A)*, *sul2*, *dfrA14*
AE1	ST38	O86:H18	D	*fimH5*	NT	bla_{OXA-1}, bla_{EC-8}	*aadA1*	*tet(B)*, *catA1*,*sul1*, *dfrA7*, *qacE*
E13	ST69	O17:H18	D	*fimH27*	CH35-27	bla_{TEM-1B},bla_{EC-8}	*aph(3")-Ib*, *aph(3')-Ia*, *aph(6)-Id*, *aadA5*	*mph(A)*, *mrx*, *tet(B)*, *sul2*, *tet(R)*, *dfrA17*
E25	ST69	O45:H16	D	*fimH27*	CH35-27	bla_{EC-8}	*aadA2*	*sul1*, *dfrA12*, *mph(A)*
K41	ST69	O45:H16	D	*fimH27*	CH35-27	bla_{EC-8}	*aac(3)-IIa*, *aadA2*, *aph(3")-Ib*, *aph(6)-Id*, *aac(3)-IIe*	*tet(A)*, *sul1*, *sul2*, *dfrA12*, *mph(A)*, *qacE*
E17	ST59	O1:H7	F	*fimH54*	CH32-54	bla_{EC-5}	-	*mdf(A)*
E21	ST155	O30:H25	B1	*fimH121*	CH4-121	bla_{EC-13}	-	-

Other antibiotic resistance genes (ARGs) include those conferring resistance to macrolides (*mph[A]*, *mrx*), sulfonamides (*sul1*, *sul2*), tetracyclines (*tet[A]*, *tet[B]*, *tet[R]*), trimethoprim (*dfrA* variants), and quaternary ammonium compounds (*qacE*)

CHtype refers to typing scheme based on *fumC* and *fimH* allele combinations

"—" indicates no gene detected

"NT" denotes non-typable (i.e., no valid allele or serotype could be assigned)

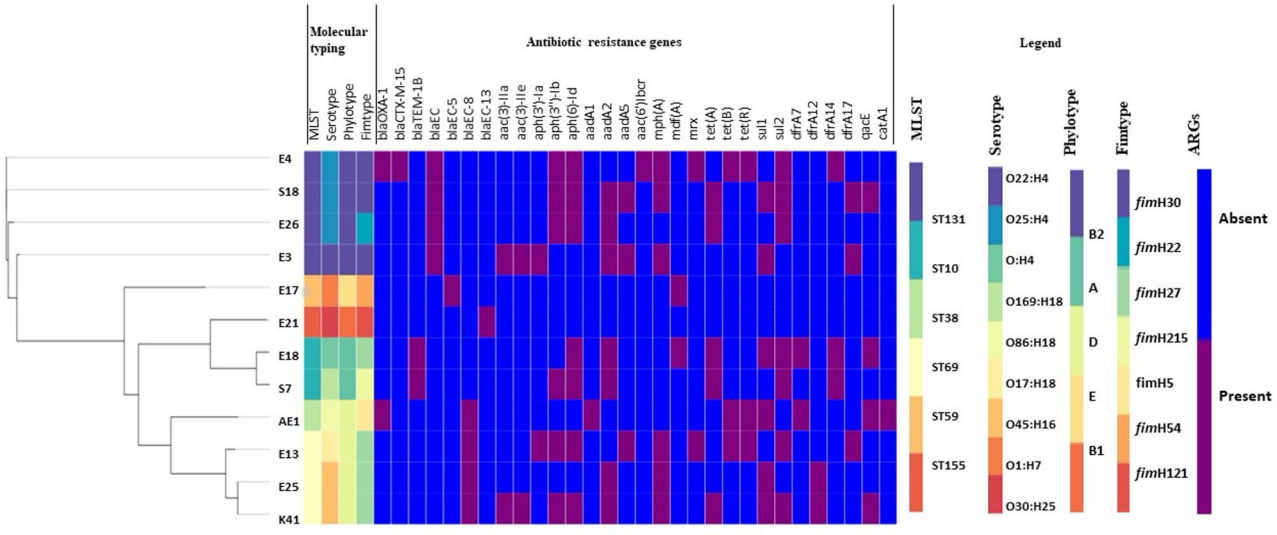

Fig. 2 The heatmap illustrates the distribution of antimicrobial resistance genes (ARGs) alongside molecular typing metadata, including MLST, serotype, phylogroup, and *fimH* type, in the MDR *E. coli* bloodstream isolates. ARG presence is shown in purple and absence in blue. Molecular typing features are color-coded according to the legend

aminoglycoside resistance were also present in 10 isolates (83.3%). The most frequently detected were *aph(6)-Id* ($n=7$), *aph(3")-Ib* ($n=6$), and *aadA5* ($n=3$). Additional aminoglycoside resistance genes included *aph(3')-Ia*($n=2$), *aac(3)-IIa* ($n=2$), *aac(3)-IIe* ($n=2$), *aadA1* ($n=1$), and *aadA2* ($n=2$) (Fig. 2).

Sulfonamide resistance genes were detected in 10 isolates (83.3%), with *sul1* ($n=7$) and *sul2* ($n=6$) being the most common. Only two isolates carried both *sul1* and

sul2. Trimethoprim resistance genes were found in nine isolates (75.0%), predominantly *dfrA17* (*n* = 3), *dfrA14* (*n* = 3), *dfrA7* (*n* = 2), and *dfrA12* (*n* = 2).

Tetracycline resistance genes were identified in seven isolates (58.3%), including *tet(A)* (*n* = 4), *tet(B)* (*n* = 3), and *tet(R)* (*n* = 2). No isolate carried both *tet(A)* and *tet(B)*; however, two isolates (16.7%) co-harbored *tet(B)* and *tet(R)* (Table 1). The quaternary ammonium compound resistance gene *qacE* was detected in four isolates (33.3%), and the phenicol resistance gene *catA1* in a single isolate. In all cases, the *qacE* allele corresponded to *qacEΔ1*, the truncated variant typically located in the 3′ conserved region of class 1 integrons; no complete *qacE* genes were identified. Notably, associations were observed between specific STs, phylogroups, and β-lactamase genes. For example, $bla_{\text{TEM-1B}}$ was consistently found among ST131 isolates belonging to phylogroup B2 and $bla_{\text{EC-8}}$ gene was restricted to phylogroup D (Table 1; Fig. 2).

Mobile genetic elements, syntenic organization, and genetic context of antimicrobial resistance genes

Plasmid replicon typing identified 35 replicons across the isolates, most frequently IncFIB (*n* = 7), IncFII (*n* = 6), and IncFIA (*n* = 5), with several Col-like replicons also detected. ARGs were considered plasmid-associated when located on the same contig as a replicon, acknowledging that definitive plasmid structures cannot be resolved using short-read data. Notably, the vast majority of isolates (91.7%) harbored multiple plasmid replicons (Table 2).

Insertion sequences (IS) and related miniature inverted-repeat transposable elements (MITEs, e.g., MITEEc1) were widely distributed, with a total of 32 IS types detected. The most prevalent elements included *MITEEc1* (*n* = 10), *ISEc38* (*n* = 9), *ISKpn8* (*n* = 7), *IS30* (*n* = 7), *ISEc10* (*n* = 6), *ISEc1* (*n* = 6), *ISEc53* (*n* = 5), *IS6100* (*n* = 5), and *IS4* (*n* = 5) (Table 2). Transposons were less common, with only two isolates carrying characterized transposons (*Tn*6170 and members of the *Tn3* family) (Table 2).

The integrase gene *intI1*, a hallmark of class 1 integrons, was detected in 9 out of 12 isolates (75.0%). It was most frequently associated with high-risk lineages, including ST131 within phylogroup B2 (*n* = 4, 33.3%) and ST69 within phylogroup D (*n* = 3, 25.0%) (Table 2). Among these, distinct gene cassette (GC) arrays were identified, with the most frequently detected configurations being *aadA5–dfrA17* (*n* = 3) and *aadA2–dfrA12* (*n* = 2). In addition, *qacEΔ1*, located in the 3′ conserved segment of class 1 integrons, co-occurred with *dfrA7* in two isolates. These encoded resistance to trimethoprim (*dfrA* genes) and aminoglycosides (*aadA* genes targeting streptomycin/spectinomycin). Importantly, all nine isolates harboring *dfrA* genes exhibited phenotypic resistance to trimethoprim-sulfamethoxazole, confirming the functional relevance of these resistance determinants.

Table 2 Sequence types, phylogroups, and mobile genetic elements of MDR *E. coli* isolates

Sample ID	MLST	Phylogroup	Mobile genetic elements			
			Plasmids replicon	Insertion sequences	Transposon	Integrase gene
E3	ST131	B2	IncFIA, IncFIB, IncFII(pRSB107),	IS*Ec10*, IS*Ec38*, IS*Ec39*, IS*30*, IS*Ec18*, MITEEc1, IS*Kpn8*, IS*Ec1*, IS*Ec53*, IS*Ec42*, IS*6100*, IS*Ecl1*, IS*Kpn34*	Tn*6170*	*intI1*
E4	ST131	B2	IncFIA, IncFIB, IncFII(pRSB107)	IS*Ecp1*, IS*Ec38*, IS*Ec53*, IS*30*, IS*Ec10*, IS*Ec1*, IS*Kpn26*, IS*5*, IS*682*, IS*6100*, IS*26*, MITEEc1, IS*5075*	Tn*3*	*intI1*
E26	ST131	B2	IncFIB, Col156, p0111	IS*Ec38*, IS*640*, IS*682*, IS*Kpn8*, IS*30*, IS*Ec18*, IS*Ec53*, IS*Ec1*, IS*Ec10*, IS*421*, IS*5*, MITEEc1, IS*Kox3*, IS*903*, IS*629*, IS*Kox3*		*intI1*
S18	ST131	B2	IncFIA, IncFIB, Col156, IncFII,	IS*6100*, IS*30*, IS*629*, IS*Ec38*, IS*Ec53*, IS*Ec1*, IS5, IS*682*, IS*Kpn8*, MITEEc1		*intI1*
E18	ST10	A	Col(MG828), Col(BS512), Col(MP18), Col8282	MITEEc1, IS*Ec37*, IS*Kpn8*, IS*421*, IS*Ec1*, IS*Kpn37*	Tn*3*	*intI1*
S7	ST10	A	Col(MG828), Col(MP18), colE5	IS26, IS*3*, IS*102*,MITEEc1, IS*100*, IS*Kpn8*, IS*Ec45*, IS*Ec30*, IS*Ec37*, IS*Ec38*	Tn*3*	
AE1	ST38	D	IncFIB, IncFII	IS*30*, IS*4*, IS*100*, IS*640* IS*Kpn8*, IS*Kpn26*, IS*Kpn37* IS*Ec1*, IS*Ec38*, IS*Ec46*, IS*609*, IS*Sfl8*, IS*5075*		*intI1*
E13	ST69	D	IncQ1, IncFII(29)	IS*21*, IS*3*, MITEEc1, IS*110*, IS*Ec38*, ISEc*42*, IS*30*, IS*4*, IS*5*		*intI1*
E25	ST69	D	IncFIA, IncFIB	IS*6100*, IS*Ec10*, MITEEc1, IS*4*, IS*Ec38*, IS*Ec46*, IS*Ec31*, IS26, IS*Sfl8*, IS*640*		*intI1*
K41	ST69	D	IncFIA, IncFIB	IS*630*, IS*Ec10*, IS*Kpn37*, IS*4*, IS*Ec46*, IS*Ec38*, IS*Ec31*, IS*6100*, IS*Sfl8*	Tn*3*	*intI1*
E17	ST59	F	IncFII(29)	IS26, MITEEc1, ISEc*45*, ISKpn*8*, ISKpn*37*, IS*4*, IS*30*, ISEc*10*, IS*100*, ISEc*53*, ISEc*31*		
E21	ST155	B1	IncB/O/K/Z, IncX1	MITEEc1, IS*3*		

MLST Multilocus sequence type, *ICE* Integrative and conjugative element (if applicable); *Inc*-type: Plasmid incompatibility group; "–" indicates absence

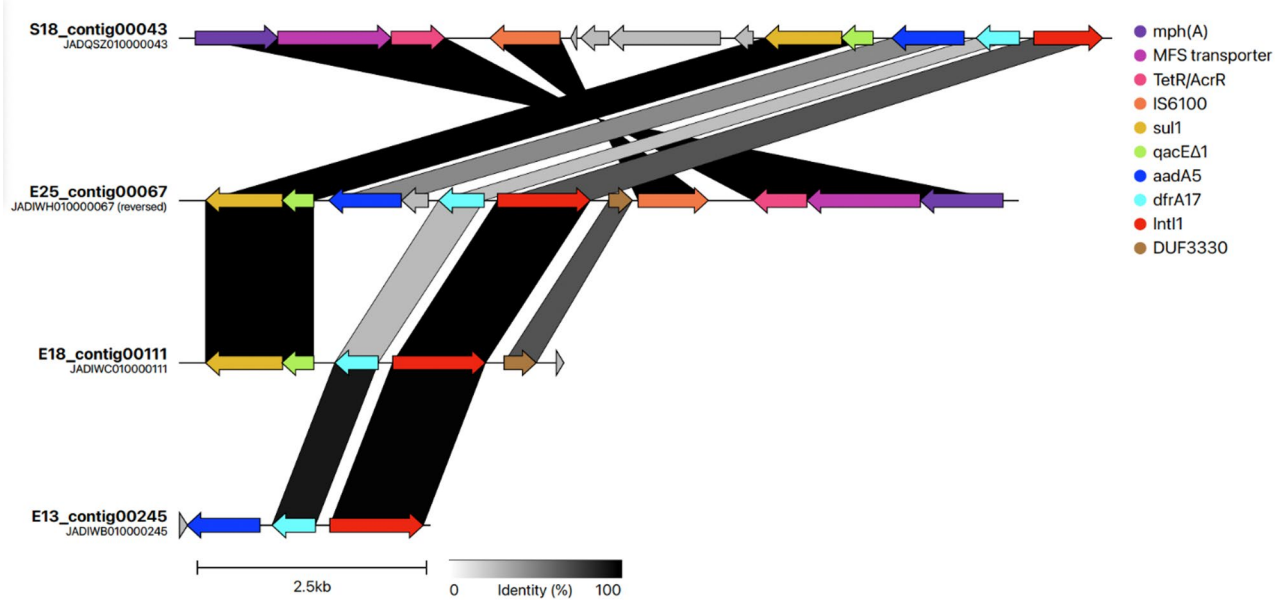

Fig. 3 Comparative visualization of integron-associated resistance regions in MDR *E. coli* isolates E13 (contig 245), E18 (contig 111), E25 (contig 67), and S18 (contig 43), displayed on a common scale. Homologous genes shared across loci are connected by shaded ribbons, with darker shading indicating higher sequence identity. The regions are shown in a standardized orientation to facilitate comparison of gene order, cassette organization, and adjacent mobile genetic elements. Shorter loci are represented by proportionally shorter backbone bars. Gene colours indicate homologous groups identified and do not represent functional categories. Arrows indicate gene orientation

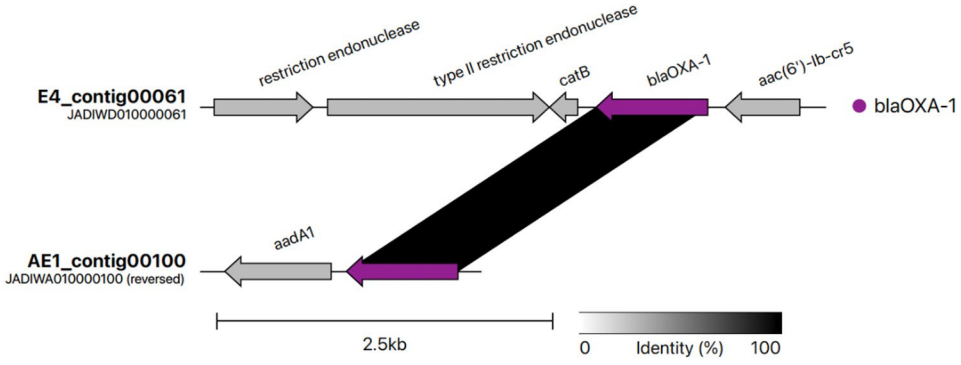

Fig. 4 Comparative linear representation of the bla_{OXA-1} genetic environment in two MDR *E. coli* isolates, AE1 (contig 100) and E4 (contig 61), and displayed on a common scale. The shared bla_{OXA-1}-containing region is connected by a shaded ribbon, with shading intensity reflecting sequence identity. The shorter AE1 locus is represented by a proportionally shorter backbone bar. Genes are coloured according to homologous group, while non-homologous genes are shown in grey. Arrows indicate gene orientation

The syntenic organization of MGEs and their association with ARGs is detailed in Table S4. Integrons exhibited structural diversity in cassette order, reflecting the activity of integrase-mediated recombination that drives insertion, excision, and rearrangement of GC. Isolate S18 carried the integron structure *mph(A)-IS6100::sul1:qacE:aadA5:dfrA17:intI1*, whereas E25 and E18 displayed rearranged or truncated variants of this cassette. E13, in contrast, showed a compact architecture with fewer associated resistance genes (Fig. 3).

The synteny and genetic context of key ARGs; $bla_{CTX-M-15}$, bla_{TEM-1B} and bla_{OXA-1} varied across the isolates (Table S4). In isolate E4, bla_{OXA-1} was chromosomally positioned adjacent to *catB* and *aac(6')-Ib-cr5*, forming part of a multiresistance region (Fig. 4); in AE1, it co-localized with *aadA1* on a plasmid related to *E. coli* plasmid pSCU-397-2 (CP054830.1) (Fig. 4). The bla_{TEM-1B} gene was observed in several isolates with diverse MGE configurations (Table S4). In E4, it co-localized with *IS91* and aminoglycoside resistance genes on a contig showing homology to the *E. coli* plasmid pLA041 (OP242256.1) (Fig. 5). In E18, bla_{TEM-1B} was part of a resistance gene cluster bounded by *sul2*, a recombinase, Tn3, and IS91, on a plasmid resembling *E. coli* plasmid pE17EC0085-3 (CP088489.1) (Fig. 5). The isolate E26 harbored bla_{TEM-1B} in association with IncFII, *pemI/*

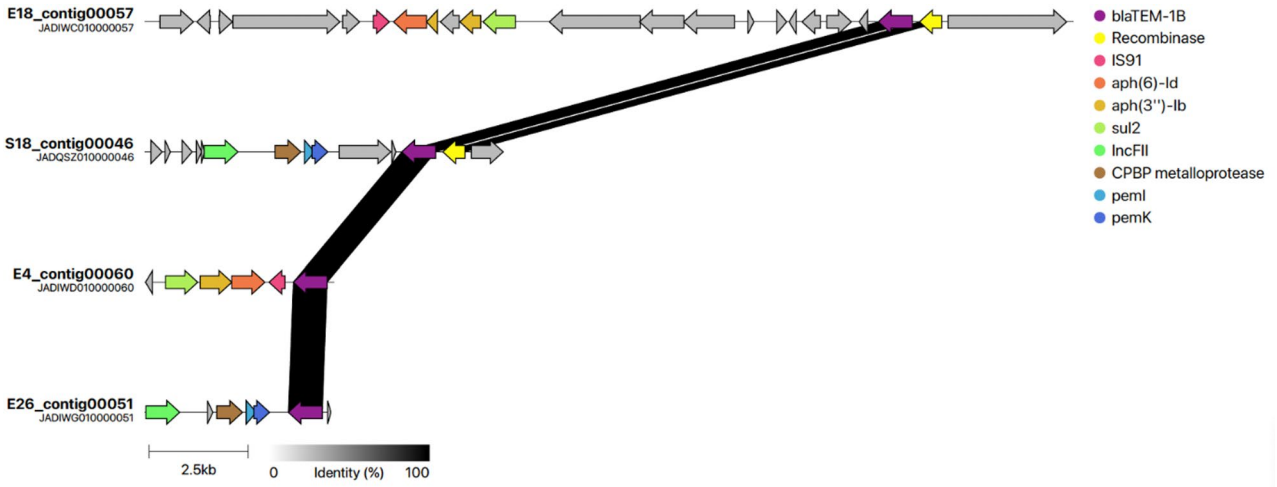

Fig. 5 Comparative visualization of bla_{TEM-1B}-associated genomic regions in MDR *E. coli* isolates E26 (contig 51), E4 (contig 60), S18 (contig 46), and E18 (contig 57) displayed on a common scale. Homologous genes are linked by shaded ribbons, with darker shading indicating higher sequence identity. The figure highlights shared and distinct features of the bla_{TEM-1B}-associated regions across isolates, including adjacent resistance-associated and plasmid-related genes. Shorter loci are shown as proportionally shorter backbone bars. Gene colours indicate homologous groups, and do not represent functional categories. Arrows indicate gene orientation

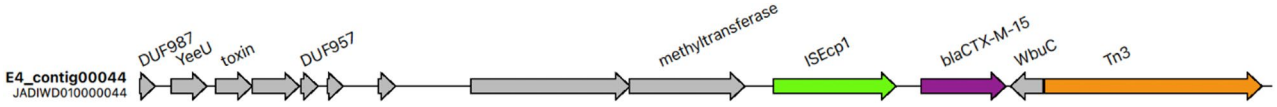

Fig. 6 Single-locus linear map of the genetic environment of $bla_{CTX-M-15}$ in MDR Escherichia coli isolate E4 (contig 44; accession no. JADIWD010000044). The $bla_{CTX-M-15}$ gene is located on a chromosomal contig and is adjacent to *ISEcp1* and a Tn3-family transposon. Green indicates antimicrobial resistance genes, orange denotes mobile genetic elements, and grey represents genetic features not directly associated with antimicrobial resistance. Arrows indicate gene orientation

pemK toxin-antitoxin genes, and *IS6*, consistent with its location on a conjugative plasmid (CP148278.1) (Fig. 5). In S18, it was located downstream of *IS1* and adjacent to a recombinase gene on a plasmid (AP018458.1) (Fig. 5). In isolate E4, $bla_{CTX-M-15}$ was located adjacent to ISEcp1 and a Tn3-family transposon, consistent with potential transposon-mediated mobilization. As this gene was identified in only one isolate, its surrounding genomic region is shown as a single-locus context map (Fig. 6) rather than a comparative synteny plot.

Virulence factors analysis

Across the 12 genomes, 56 virulence-associated genes were detected (Table S5). Several genes represented core *E. coli* traits, including *ompT*, *fimH*, and siderophore-associated loci such as *sitA*, while others reflected ExPEC-associated pathogenicity markers. Adhesion-related genes included *fimH*, *iha*, *afaABCD*, *papA* (alleles *papA_F9*, *papA_F13*), *papC*, *yfcV*, and *lpfA*, supporting the presence of both fimbrial and afimbrial adhesion systems typically enriched in extraintestinal pathogenic lineages. Iron acquisition systems were widespread and included aerobactin genes (*iucC*, *iutA*), yersiniabactin-associated loci (*fyuA*, *irp2*), and the heme uptake gene *chuA*, features commonly associated with invasive ExPEC strains. Capsule biosynthesis genes identified across isolates included *kpsE*, *kpsMII*, and specific group II capsule variants (*kpsMII_K1*, *kpsMII_K5*, *kpsMII_K24*) as well as *neuC*, consistent with established markers of serum resistance. Toxin-associated genes detected included *hlyA*, *hlyE*, *senB*, and *cnf1*, together with additional determinants linked to invasion (*ibeA*, *tia*) and serum resistance (*traT*, *iss*). Autotransporter proteins such as *pic*, *sat*, *vat*, *air*, and *hra* were also present (Table S5). Several virulence genes co-occurred with insertion sequences, including IS3-, IS30-, ISL3-, and IS91-family elements (Table S6). For example, *senB* was most frequently associated with IS91-type elements and displayed 98–100% identity to plasmid-encoded *senB* sequences deposited in GenBank (Table S6).

Phylogenetic analysis and metadata insights

The core-genome phylogenetic tree revealed distinct clustering patterns based on ST, geographic origin, and year of isolation (Fig. 7 and Table S7). The globally recognized ST131 isolates from this study (E4, E3, E26, S18) clustered closely with other ST131 strains from South Africa, Malawi, and Tanzania, most of which

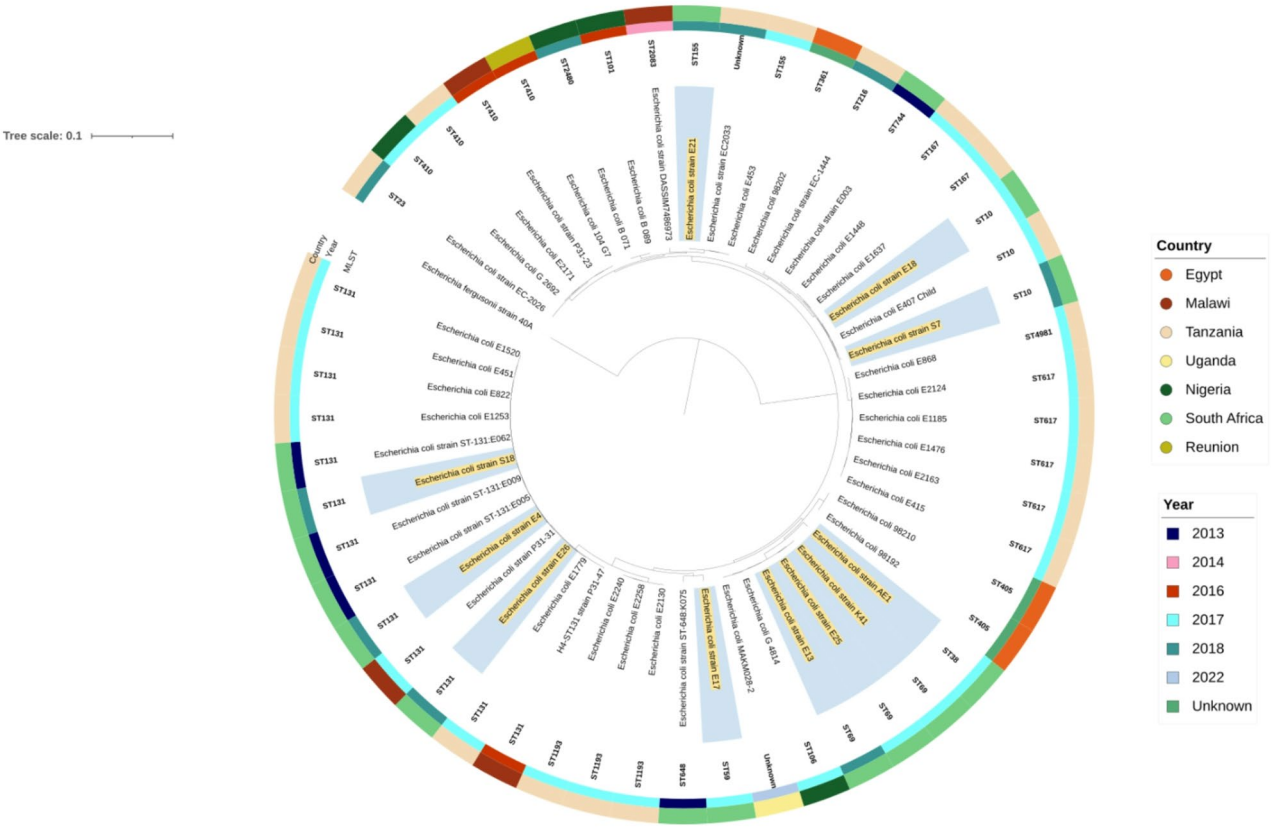

Fig. 7 Maximum likelihood circular phylogenetic tree of *E. coli* isolates recovered from human bloodstream infections across African countries. The tree was generated from the core genome alignment of 51 *E. coli* genomes retrieved from the BV-BRC database and annotated using iTOL. *E. coli fergusonii* strain 40 A served as the outgroup to root the tree. The concentric colored rings represent key metadata: the innermost ring shows Multilocus sequence type (MLST), the middle ring indicates the country of isolation, and the outer ring denotes the year of isolation. Isolates from this study are marked with a yellow background

were isolated between 2013 and 2018. The ST155 isolate (E21) grouped with a bloodstream isolate from Tanzania (2018). Other high-risk lineages from this study, including ST69 (E25, K41) and ST38 (AE1), grouped closely with ST106 and an untyped strain from Nigeria and Uganda, for which the available metadata indicated collection years of 2017 and 2022, respectively. The ST10 isolates (E18, S7) from this study clustered with an ST167 isolate from Tanzania (2017). In contrast, the ST59 isolate (E17) diverged from the ST131 clade and aligned more closely with a South African bloodstream isolate collected in 2013 (Fig. 7).

Discussion

WGS of MDR E. coli isolates from BSIs in South Africa revealed considerable genomic diversity across sequence types, serotypes, and phylogenetic backgrounds. Both pandemic and regionally emerging lineages were represented, including the high-risk clones ST131, ST69, ST10, and ST38.

Among the 12 isolates sequenced, ST131/phylogroup B2 was the most common lineage (33.3%), consistent with its recognized role as a high-risk ExPEC clone [23]. This pattern mirrors recent genomic surveillance, where ST131-O25:H4-H30 was reported as the leading cause of *E. coli* bloodstream infections [14, 24, 25]. In our study, these ST131-H30 isolates demonstrated both extensive resistance phenotypes and the highest burden of acquired resistance genes, reinforcing their designation as high-risk clones. The remaining ST131 isolate (E26) harbored the *fimH22* allele, representing a less common but clinically relevant sublineage [23, 26]. Beyond ST131, we identified representatives of other globally distributed pathogenic high-risk *E. coli* lineages. These included ST69/phylogroup D (25%), ST10/phylogroup A (16.7%), and a single isolate of ST38/phylogroup D. This diversity aligns with global reports that have identified a similar dominance of key lineages among *E. coli* bloodstream isolates [14, 23–27]. Moreover, these epidemiologically significant clonal groups, characterized by broad host range and ecological versatility, have been recovered from human, animal, and environmental sources [28]. Importantly, our CH typing data revealed eight distinct CH types, with CH40-30 and CH35-27 being the

most dominant, both associated with ST131 and ST69, respectively. These CH-types correspond with previously described MDR sublineages and support the notion of convergent evolution within high-risk clones [29–31]. Taken together, our findings highlight the regional circulation of pandemic *E. coli* lineages, notably ST131-H30, within South Africa's healthcare system, while also pointing to the co-existence of genetically diverse and potentially emerging clones such as ST69, ST10 and ST38.

The resistance gene profiles of the *E. coli* isolates reveal the accumulation of diverse ARGs across phylogenetically distinct lineages. The widespread detection of β-lactamases, particularly ESBLs in conjunction with aminoglycoside, sulfonamides, tetracycline, and trimethoprim resistance determinants suggests suggests sustained antimicrobial selection and co-selection within clinical settings. Beyond this diversity, the non-random distribution of specific ARGs among defined sequence types and phylogroups [32]. In our study, ST131 and ST69 isolates co-occurred with multi-layered resistance profiles. While similar patterns have been reported globally, our data are limited to four and two isolates, respectively, and should be interpreted as preliminary observations rather than definitive trends. These lineages not only co-harbored β-lactamases with additional ARGs but also frequently encoded them in syntenic blocks with insertion sequences and integrons, reflecting well-documented mechanisms of ARG mobilization [6]. The detection of *qacEΔ1* in several isolates indicates the presence of class 1 integrons that may carry additional ARGs beyond those captured by routine phenotypic testing. As a truncated remnant of *qacE* located in the 3′ conserved segment, *qacEΔ1* is better interpreted as a genomic marker of class 1 integrons than as a functional resistance determinant [33]. Its co-occurrence with multidrug resistance genes highlights the integron- and MGE-associated contexts through which high-risk *E. coli* clones accumulate and maintain accessory genes under antimicrobial and biocide pressure [34, 35].

The structural characterization of integrons among the isolates revealed notable syntenic variability, reflecting their function as genetic platforms for capturing and expressing resistance cassettes, and their association with mobile elements or homologous recombination events that facilitate the dissemination of AMR genes [36] (Fig. 3). Where detected, class 1 integron-associated regions carried the canonical *intI1* integrase gene, defining the core scaffold of class 1 integrons, the downstream gene cassettes, insertion elements, and chromosomal or plasmid contexts displayed significant heterogeneity [37]. However, in some isolates, intI1 was not recovered on the same contig, most likely due to short-read assembly fragmentation. In isolate S18, a composite integron structure (*mph(A)-sul1-qacE-aadA5-dfrA17*) bracketed by IS*6100* elements was observed, recapitulating conserved resistance clusters previously identified in both clinical and zoonotic *E. coli* reservoirs [38–42]. This structure mirrors configurations found in both clinical and animal-associated *E. coli*, further reinforcing the hypothesis of shared reservoirs and frequent horizontal transmission events across ecological boundaries, and underscoring the critical need for a One-Health AMR surveillance framework. In contrast, isolates E25 and E18 harbored truncated or rearranged integrons, exhibiting disrupted cassette arrays and divergent flanking elements a pattern reminiscent of integron remodeling observed in some drug-resistant bacteria [43, 44]. Their integration into plasmid scaffolds carrying IS*6100* and Tn*3* transposons, well-established mediators of ARG mobility emphasizes the plasticity of these elements in facilitating both clonal expansion and lateral gene flow across Enterobacterales.

This mosaic genetic complexity is further exemplified by the distinct syntenic environments of key β-lactamase genes. In isolate E4, $bla_{\text{CTX-M-15}}$ was chromosomally integrated between IS*Ecp1* and Tn*3*, forming a composite transposition unit mirroring the IS*Ecp1*-$bla_{\text{CTX-M-15}}$ module previously reported in clinical and environmental isolates of *E. coli*, *Enterobacter cloacae*, and *Klebsiella pneumoniae* from Australia, Zambia, Belgium, and Japan [45–48]. In contrast, the β-lactamase, $bla_{\text{TEM-1B}}$ displayed diverse architectures across isolates: in S18, it co-localized with IS1 and recombinase genes on a plasmid; in E26, the gene was located on the same contig as an IncFII replicon and flanked by IS6 and the *pemI/pemK* toxin–antitoxin system, a configuration commonly associated with stable plasmid maintenance [42, 49–51]. Meanwhile, $bla_{\text{OXA-1}}$ was identified in both chromosomal (E4) and plasmid (AE1) contexts, co-occurring with *aac(6')-Ib-cr* and *aadA1*, respectively reflecting conserved resistance clusters widely reported in global *E. coli* lineages such as ST131, ST10, ST648, and ST410 [42, 50]. These layered configurations spanning chromosomal insertions, integron scaffolds, and conjugative plasmid contexts highlight the synergistic interactions among MGEs, resistance genes, and genomic stability systems [52, 53]. Although several isolates shared closely related genomic backgrounds and overlapping ARG/MGE configurations, these patterns are suggestive of, but do not prove, recent transmission. Given the substantial role of plasmid-mediated horizontal gene transfer in shaping AMR in *E. coli*, similar genomic signatures may arise through shared mobile elements rather than clonal spread. Accordingly, our interpretations focus on the genomic contexts observed rather than inferring direct dissemination events.

The virulence gene repertoire identified in these isolates reflects the combination of pathogenic strategies that support bloodstream invasion, immune evasion, and

persistence within host tissues [54, 55]. The widespread detection of adhesins such as *fimH*, serum resistance determinants including *iss* and *traT*, and group II capsule biosynthesis loci (*kpsE*, *kpsMTII*) underscores their established contribution to ExPEC survival in extraintestinal sites [56]. In addition, the presence of secreted autotransporter proteins (*sat*, *vat*) and toxins (*hlyA*, *cnf1*) is consistent with virulence profiles commonly observed among extraintestinal pathogenic *E. coli* lineages, some of which display features of hybrid pathotypes [56, 57]. These observations suggest the persistence of selective pressures that enable the co-maintenance of virulence and antimicrobial resistance determinants within successful clones. Notably, several virulence-associated genes were co-located with mobile genetic elements, raising concern about the potential for linked acquisition or dissemination of fitness-enhancing and resistance traits, which may further complicate clinical management of invasive infections.

The observed clustering of ST131 isolates with counterparts across Africa, spanning 2013–2022, suggests regional circulation; however, given the small number of isolates analyzed here, these findings should be considered preliminary. This widespread distribution underscores the fitness and adaptability of ST131 and its continued threat to public health systems [15, 16, 23]. Additionally, the clustering of ST155 and ST69 isolates with Tanzanian and Nigerian strains, respectively, may reflect shared evolutionary backgrounds or historical links; however, the absence of a broader comparative dataset, including genomes from additional sources and regions, limits definitive interpretation. The proximity of ST69 to the ST106 clonal complex, both carrying β-lactamases, highlights the genomic fluidity enabled by horizontal gene transfer. Phylogenetically distinct lineages like ST10 and ST59, found near older strains, suggest the presence of long-standing reservoirs and potential re-emergence routes. These findings emphasize the need for integrated, longitudinal genomic surveillance across African countries to monitor clonal dynamics, resistance evolution, and inform region-specific control strategies before resistant lineages silently become entrenched.

This study is limited by the small number of MDR isolates from a restricted hospital setting, which reduces generalizability. Broader surveillance across multiple hospitals, combined with integrated phenotypic–genomic analyses and key clinical metadata, will be needed to better define AMR dynamics and clinical relevance [58]. Moreover, including animal and environmental sources will further illuminate One Health transmission pathways and the regional spread of high-risk clones [59, 60]. We acknowledge that short-read sequencing could not resolve complete plasmid architectures; therefore, plasmid-associated ARGs were inferred from co-localization with plasmid replicons on the same contigs. In addition, phenotypic colistin susceptibility testing was not performed, and no conclusions on colistin resistance could be made beyond the absence of *mcr* genes in the genomic data.

Conclusions

This study reveals a striking level of genomic diversity among MDR *E. coli* isolates recovered from bloodstream infections in a South African healthcare setting. High-risk international clones including ST131 (phylogroup B2), ST69 (phylogroup D), ST10 (phylogroup A), and ST38 were identified, underscoring the circulation of globally recognized pathogenic *E. coli* lineages within a local clinical context. These clones harbored an array of β-lactamase genes, most notably $bla_{\text{TEM-1B}}$, $bla_{\text{OXA-1}}$ and $bla_{\text{CTX-M-15}}$, as well as other ARGs, reflecting complex and multidrug resistance genes. Notably, many ARGs were associated with diverse MGEs, including class 1 integrons, insertion sequences (IS*91*, IS*Ecp1*, IS*6100*), and transposons (Tn*3*, Tn*6170*) and were frequently linked to IncF-type plasmids. These mobile elements frequently co-harbored multiple ARGs within conserved syntenic frameworks, consistent with the mobilization of shared resistance regions through homologous recombination, which can result in identical genetic structures appearing in otherwise unrelated strains. This structural arrangement enhances the likelihood of co-selection and co-dissemination under antimicrobial pressure. Comparative mapping suggested putative syntenic arrangements of multiresistance regions. However, these interpretations are limited by short-read assemblies, and definitive resolution would require long-read sequencing. The co-circulation of such mosaic, high-risk lineages heightens the threat of untreatable bloodstream infections and underscores the progressive erosion of last-resort antibiotics. Together, these findings highlights the urgent need for enhanced genomic surveillance frameworks in sub-Saharan Africa to track the emergence and dissemination of MDR pathogens. The integration of pathogenomics into routine surveillance programs is vital for informing infection control strategies, guiding empirical treatment protocols, and mitigating the public health threat posed by high-risk MDR *E. coli* clones in resource-limited healthcare systems.

Abbreviations

AMR	Antimicrobial Resistance
BSIs	Bloodstream Infections
CDS	Coding Sequence
E. coli	Escherichia coli
ESBLs	Extended-Spectrum β-Lactamases
GFF	General Feature Format
iTOL	Interactive Tree of Life
Inc	Incompatibility (plasmid replicon type)

IS	Insertion Sequence
intI1	Integrase gene of class 1 integrons
MGEs	Mobile Genetic Elements
MDR	Multidrug-Resistant
MLST	Multilocus Sequence Typing
ST	Sequence Type
Tn	Transposon
WGS	Whole-Genome Sequencing
WHO	World Health Organization

Supplementary Information

The online version contains supplementary material available at https://doi.org/10.1186/s12920-026-02349-y.

Supplementary Material 1.

Acknowledgements
We are grateful to Sumayya Haffejee of the National Health Laboratory Services for her assistance during sample collection and obtaining demographic data.

Authors' contributions
BH, EEAY, SYE, and DGA co-conceptualized the study. BE was responsible for sample collection and laboratory processing. BH and DGA drafted the original manuscript. BH, EEAY, and DGA conducted the data analysis. AI performed whole-genome sequencing of the isolates. AI, SYE, and DGA provided supervision, validated the results, and critically reviewed the manuscript. All authors (BH, EEAY, AI, SYE, and DGA) contributed to manuscript review and editing, and approved the final version for submission.

Funding
This work was supported by the South African Research Chairs Initiative of the Department of Science and Technology and the National Research Foundation of South Africa (Grant No. 98342), the South African Medical Research Council (SAMRC), the UK Medical Research Council (UK MRC) through the Newton Fund, and the SAMRC Self-Initiated Research Grant. Additional support was provided by the College of Health Sciences, University of KwaZulu-Natal, South Africa.

Data availability
The whole-genome sequence data generated in this study have been deposited in GenBank under BioProject accession number **PRJNA669537** . All other relevant data supporting the findings of this study are included within the main manuscript and its supplementary materials.

Declarations

Ethics approval and consent to participate
This study was conducted in accordance with the ethical principles outlined in the Declaration of Helsinki. Ethical clearance was obtained from the Biomedical Research Ethics Committee of the University of KwaZulu-Natal (Reference: BCA444/16). Voluntary, informed written consent was obtained from participating patients and staff.

Competing interests
The authors declare no competing interests.

Consent for publication
Not applicable.

Author details
[1]Antimicrobial Research Unit, College of Health Sciences, University of KwaZulu-Natal, Durban, South Africa
[2]Department of Pharmaceutical Sciences, School of Pharmacy, Central University, P. O. Box 2305, Miotso, Ghana
[3]Sequencing Core Facility, Division of the National Health Laboratory Service, National Institute for Communicable Diseases, Johannesburg 2193, South Africa
[4]School of Pharmacy, University of Jordan, Amman 11942, Jordan

Received: 5 July 2025 / Accepted: 20 March 2026
Published online: 25 March 2026

References

1. ECDC. European Centre for Disease Prevention and Control. Antimicrobial resistance in the EU/EEA (EARS-Net) - Annual Epidemiological Report 2019. Stockholm: ECDC. 2020. Antimicrobial resistance in the EU/EEA (EARS-Net). 2020;174.
2. Word Health Organization. Global Antimicrobial Resistance and Use Surveillance System (GLASS) Report 2022. 2022;33.
3. Niazi E, Mponponsuo K, Somayaji R, Rennert-May E, Conly J, Gregson D, et al. 224. Evaluating the Epidemiology of Bloodstream Infections: A Population-Based Study. Open Forum Infect Dis. 2021. https://doi.org/10.1093/ofid/ofab466.426. 8 Supplement_1.
4. collaborators A, Darboe S, Carvalheiro C, Haller S, Dunachie S, Haines-Woodhouse G et al. Articles Global burden of bacterial antimicrobial resistance in 2019: a systematic analysis Antimicrobial Resistance Collaborators*. Lancet. 2022;399.
5. Kariuki S, Kering K, Wairimu C, Onsare R, Mbae C. Antimicrobial Resistance Rates and Surveillance in Sub-Saharan Africa: Where Are We Now? Infect Drug Resist. 2022;15. https://doi.org/10.2147/IDR.S342753.
6. Castanheira M, Simner PJ, Bradford PA. Extended-spectrum β-lactamases: An update on their characteristics, epidemiology and detection. JAC-Antimicrobial Resist. 2021;3. https://doi.org/10.1093/jacamr/dlab092.
7. Tamma PD, Aitken SL, Bonomo RA, Mathers AJ, Van Duin D, Clancy CJ. Infectious Diseases Society of America Guidance on the Treatment of Extended-Spectrum β-lactamase Producing Enterobacterales (ESBL-E), Carbapenem-Resistant Enterobacterales (CRE), and Pseudomonas aeruginosa with Difficult-to-Treat Resistance (DTR-P. aeruginosa). Clin Infect Dis. 2021;72. https://doi.org/10.1093/cid/ciab295.
8. Woerther PL, Angebault C, Lescat M, Ruppé E, Skurnik D, El Mniai A, et al. Emergence and dissemination of extended-spectrum β-lactamase-producing Escherichia coli in the community: Lessons from the study of a remote and controlled population. J Infect Dis. 2010;202. https://doi.org/10.1086/654883.
9. De Angelis G, Giacomo P, Del, Posteraro B, Sanguinetti M, Tumbarello M. Molecular mechanisms, epidemiology, and clinical importance of β-lactam resistance in enterobacteriaceae. Int J Mol Sci. 2020;21. https://doi.org/10.3390/ijms21145090.
10. Bush K, Bradford PA. β-Lactams and β-Lactamase Inhibitors: An Overview. Cold Spring Harb Perspect Med. 2016;6:a025247. https://doi.org/10.1101/cshperspect.a025247.
11. Bush K. Past and Present Perspectives on β-Lactamases. Antimicrob Agents Chemother. 2018;62. https://doi.org/10.1128/AAC.01076-18.
12. Durão P, Balbontín R, Gordo I. Evolutionary Mechanisms Shaping the Maintenance of Antibiotic Resistance. Trends Microbiol. 2018;26. https://doi.org/10.1016/j.tim.2018.01.005.
13. Partridge SR, Kwong SM, Firth N, Jensen SO. Mobile Genetic Elements Associated with Antimicrobial Resistance. Clin Microbiol Rev. 2018;31:1–61. https://doi.org/10.1128/CMR.00088-17.
14. Santona A, Sumbana JJ, Fiamma M, Deligios M, Taviani E, Simbine SE, et al. High-risk lineages among extended-spectrum β-lactamase-producing Escherichia coli from extraintestinal infections in Maputo Central Hospital, Mozambique. Int J Antimicrob Agents. 2022;60. https://doi.org/10.1016/j.ijantimicag.2022.106649.
15. Pitout JDD, DeVinney R. Escherichia coli ST131: A multidrug-resistant clone primed for global domination. F1000Research. 2017;6. https://doi.org/10.12688/f1000research.10609.1.
16. Stoesser N, Sheppard AE, Pankhurst L, de Maio N, Moore CE, Sebra R et al. Evolutionary history of the global emergence of the Escherichia coli epidemic clone ST131. mBio. 2016;7. https://doi.org/10.1128/mBio.02162-15
17. Duprilot M, Baron A, Blanquart F, Dion S, Pouget C, Lettéron P, et al. Success of Escherichia coli O25b:H4 sequence type 131 clade C associated with a decrease in virulence. Infect Immun. 2020;88. https://doi.org/10.1128/IAI.00576-20.
18. Shaik S, Ranjan A, Tiwari SK, Hussain A, Nandanwar N, Kumar N, et al. Comparative genomic analysis of globally dominant ST131 clone with other epidemiologically successful extraintestinal pathogenic escherichia coli (ExPEC) lineages. mBio. 2017;8. https://doi.org/10.1128/mBio.01596-17.

19. Kajumbula HM, Amoako DG, Tessema SK, Aworh MK, Chikuse F, Okeke IN, et al. Enhancing clinical microbiology for genomic surveillance of antimicrobial resistance implementation in Africa. Antimicrob Resist Infect Control. 2024;13. https://doi.org/10.1186/s13756-024-01472-8.
20. Nnah EP, Asante J, Amoako DG, Abia ALK, Essack SY. Antibiotic-resistant Escherichia coli (E. coli) at one health interfaces in Africa: A scoping review. Sci Total Environ. 2025;958. https://doi.org/10.1016/j.scitotenv.2024.177580.
21. EUCAST. The European Committee on Antimicrobial Susceptibility Testing. Breakpoint tables for interpretation of MICs and zone diameters, version 8.0. 2017. 2017. http://www.eucast.org/clinical_breakpoints/
22. Magiorakos AP, Srinivasan A, Carey RB, Carmeli Y, Falagas ME, Giske CG, et al. Multidrug-resistant, extensively drug-resistant and pandrug-resistant bacteria: An international expert proposal for interim standard definitions for acquired resistance. Clin Microbiol Infect. 2012;18:268–81. https://doi.org/10.1111/j.1469-0691.2011.03570.x.
23. Nicolas-Chanoine MH, Bertrand X, Madec JY. Escherichia coli st131, an intriguing clonal group. Clin Microbiol Rev. 2014;27. https://doi.org/10.1128/CMR.00125-13.
24. Du X, Huang J, Wang D, Zhu Y, Lv H, Li X. Whole genome sequence of an Escherichia coli ST131 strain isolated from a patient with bloodstream infection in China co-harbouring blaKPC-2, blaCTX-M-3, blaCTX-M-14, qnrS1, aac(3)-Ila and aac(6')-Ib-cr genes. J Global Antimicrob Resist. 2020;22. https://doi.org/10.1016/j.jgar.2020.06.027.
25. Li R, Xu H, Tang H, Shen J, Xu Y. The Characteristics of Extended-Spectrum β-Lactamases (ESBLs)-Producing Escherichia coli in Bloodstream Infection. Infect Drug Resist. 2023;16. https://doi.org/10.2147/IDR.S400170.
26. Boll EJ, Overballe-Petersen S, Hasman H, Roer L, Ng K, Scheutz F, et al. Emergence of enteroaggregative escherichia coli within the ST131 lineage as a cause of extraintestinal infections. mBio. 2020;11. https://doi.org/10.1128/mBio.00353-20.
27. Peirano G, Pitout JDD. Extended-Spectrum β-Lactamase-Producing Enterobacteriaceae: Update on Molecular Epidemiology and Treatment Options. Drugs. 2019;79. https://doi.org/10.1007/s40265-019-01180-3.
28. Kocsis B, Gulyás D, Szabó D. Emergence and Dissemination of Extraintestinal Pathogenic High-Risk International Clones of Escherichia coli. Life. 2022;12. https://doi.org/10.3390/life12122077.
29. Tchesnokova V, Billig M, Chattopadhyay S, Linardopoulou E, Aprikian P, Roberts PL, et al. Predictive diagnostics for Escherichia coli infections based on the clonal association of antimicrobial resistance and clinical outcome. J Clin Microbiol. 2013;51. https://doi.org/10.1128/JCM.00984-13.
30. Flament-Simon SC, Nicolas-Chanoine MH, García V, Duprilot M, Mayer N, Alonso MP, et al. Clonal structure, virulence factor-encoding genes and antibiotic resistance of Escherichia coli, causing urinary tract infections and other extraintestinal infections in humans in spain and france during 2016. Antibiotics. 2020;9. https://doi.org/10.3390/antibiotics9040161.
31. Duan Y, Gao H, Zheng L, Liu S, Cao Y, Zhu S, et al. Antibiotic Resistance and Virulence of Extraintestinal Pathogenic Escherichia coli (ExPEC) Vary According to Molecular Types. Front Microbiol. 2020;11. https://doi.org/10.3389/fmicb.2020.598305.
32. Holland MS, Nobrega D, Peirano G, Naugler C, Church DL, Pitout JDD. Molecular epidemiology of Escherichia coli causing bloodstream infections in a centralized Canadian region: a population-based surveillance study. Clin Microbiol Infect. 2020;26. https://doi.org/10.1016/j.cmi.2020.02.019.
33. Slipski CJ, Jamieson-Datzkiw TR, Zhanel GG, Bay DC. Characterization of proteobacterial plasmid integron-encoded qac efflux pump sequence diversity and quaternary ammonium compound antiseptic selection in Escherichia coli grown planktonically and as biofilms. Antimicrob Agents Chemother. 2021;65. https://doi.org/10.1128/AAC.01069-21.
34. Sakalauskienė GV, Malcienė L, Stankevičius E, Radzevičienė A. Unseen Enemy: Mechanisms of Multidrug Antimicrobial Resistance in Gram-Negative ESKAPE Pathogens. Antibiotics. 2025;14. https://doi.org/10.3390/antibiotics14010063.
35. Mcnally A, Oren Y, Kelly D, Pascoe B, Dunn S, Sreecharan T et al. Combined Analysis of Variation in Core, Accessory and Regulatory Genome Regions Provides a Super-Resolution View into the Evolution of Bacterial Populations. 2016;:1–16. https://doi.org/10.5061/dryad.d7d71
36. Baquero F, Martínez JL, Lanza VF, Rodríguez-Beltrán J, Galán JC, San Millán A, et al. Evolutionary Pathways and Trajectories in Antibiotic Resistance. Clin Microbiol Rev. 2021;34. https://doi.org/10.1128/CMR.00050-19.
37. Gillings MR, Integrons. Past, Present, and Future. Microbiol Mol Biol Rev. 2014;78. https://doi.org/10.1128/mmbr.00056-13.
38. Domingues S, da Silva GJ, Nielsen KM, Integrons. Mob Genet Elem. 2012;2:211–23. https://doi.org/10.4161/mge.22967.
39. Huang J, Lan F, Lu Y, Li B. Characterization of Integrons and Antimicrobial Resistance in Escherichia coli Sequence Type 131 Isolates. Can J Infect Dis Med Microbiol. 2020;2020. https://doi.org/10.1155/2020/3826186.
40. Toleman MA, Bennett PM, Walsh TR. IS CR Elements: Novel Gene-Capturing Systems of the 21st Century? Microbiol Mol Biol Rev. 2006;70. https://doi.org/10.1128/mmbr.00048-05.
41. Poirel L, Naas T, Nordmann P. Genetic support of extended-spectrum β-lactamases. Clin Microbiol Infect. 2008;14(SUPPL 1). https://doi.org/10.1111/j.1469-0691.2007.01865.x.
42. Mbelle NM, Feldman C, Osei Sekyere J, Maningi NE, Modipane L, Essack SY. The Resistome, Mobilome, Virulome and Phylogenomics of Multidrug-Resistant Escherichia coli Clinical Isolates from Pretoria, South Africa. Sci Rep. 2019;9:16457. https://doi.org/10.1038/s41598-019-52859-2.
43. Kubomura A, Sekizuka T, Onozuka D, Murakami K, Kimura H, Sakaguchi M, et al. Truncated Class 1 Integron Gene Cassette Arrays Contribute to Antimicrobial Resistance of Diarrheagenic Escherichia coli. Biomed Res Int. 2020;2020. https://doi.org/10.1155/2020/4908189.
44. Mazel D, Integrons. Agents of bacterial evolution. Nat Rev Microbiol. 2006;4. https://doi.org/10.1038/nrmicro1462.
45. Zong Z, Ginn AN, Dobiasova H, Iredell JR, Partridge SR. Different IncI1 plasmids from Escherichia coli carry ISEcp1-blaCTX-M-15 associated with different Tn2-derived elements. Plasmid. 2015;80. https://doi.org/10.1016/j.plasmid.2015.04.007.
46. Shawa M, Furuta Y, Mulenga G, Mubanga M, Mulenga E, Zorigt T, et al. Novel chromosomal insertions of ISEcp1-bla CTX-M-15 and diverse antimicrobial resistance genes in Zambian clinical isolates of Enterobacter cloacae and Escherichia coli. Antimicrob Resist Infect Control. 2021;10. https://doi.org/10.1186/s13756-021-00941-8.
47. Smet A, van Nieuwerburgh F, Vandekerckhove TTM, Martel A, Deforce D, Butaye P, et al. Complete nucleotide sequence of CTX-M-15-plasmids from clinical Escherichia coli isolates: Insertional events of transposons and insertion sequences. PLoS ONE. 2010;5. https://doi.org/10.1371/journal.pone.0011202.
48. Gomi R, Yamamoto M, Tanaka M, Matsumura Y. Chromosomal integration of blaCTX-M genes in diverse Escherichia coli isolates recovered from river water in Japan. Curr Res Microb Sci. 2022;3. https://doi.org/10.1016/j.crmicr.2022.100144.
49. Rozwandowicz M, Brouwer MSM, Fischer J, Wagenaar JA, Gonzalez-Zorn B, Guerra B, et al. Plasmids carrying antimicrobial resistance genes in Enterobacteriaceae. J Antimicrob Chemother. 2018;73:1121–37. https://doi.org/10.1093/jac/dkx488.
50. Asare Yeboah EE, Agyepong N, Mbanga J, Amoako DG, Abia ALK, Ismail A, et al. Genomic characterization of multi drug resistant ESBL-producing Escherichia coli isolates from patients and patient environments in a teaching hospital in Ghana. BMC Microbiol. 2024;24. https://doi.org/10.1186/s12866-024-03406-1.
51. Kamruzzaman M, Wu AY, Iredell JR. Biological functions of type ii toxin-antitoxin systems in bacteria. Microorganisms. 2021;9. https://doi.org/10.3390/microorganisms9061276.
52. Mazzamurro F, Chirakadavil JB, Durieux I, Poiré L, Plantade J, Ginevra C, et al. Intragenomic conflicts with plasmids and chromosomal mobile genetic elements drive the evolution of natural transformation within species. PLoS Biol. 2024. https://doi.org/10.1371/journal.pbio.3002814. 22 10 October.
53. Che Y, Yang Y, Xu X, Brinda K, Polz MF, Hanage WP, et al. Conjugative plasmids interact with insertion sequences to shape the horizontal transfer of antimicrobial resistance genes. Proc Natl Acad Sci U S A. 2021;118. https://doi.org/10.1073/pnas.2008731118.
54. Worley J. Immune evasion and persistence in enteric bacterial pathogens. Gut Microbes. 2023;15. https://doi.org/10.1080/19490976.2022.2163839.
55. Pakbin B, Brück WM, Rossen JWA. Virulence factors of enteric pathogenic Escherichia coli: A review. Int J Mol Sci. 2021;22. https://doi.org/10.3390/ijms22189922.
56. Sarowska J, Futoma-Koloch B, Jama-Kmiecik A, Frej-Madrzak M, Ksiazczyk M, Bugla-Ploskonska G, et al. Virulence factors, prevalence and potential transmission of extraintestinal pathogenic Escherichia coli isolated from different sources: recent reports. Gut Pathog. 2019;11:10. https://doi.org/10.1186/s13099-019-0290-0.
57. Sora VM, Meroni G, Martino PA, Soggiu A, Bonizzi L, Zecconi A. Extraintestinal pathogenic escherichia coli: Virulence factors and antibiotic resistance. Pathogens. 2021;10. https://doi.org/10.3390/pathogens10111355.
58. Waddington C, Carey ME, Boinett CJ, Higginson E, Veeraraghavan B, Baker S. Exploiting genomics to mitigate the public health impact of antimicrobial

resistance. Genome Med. 2022;14. https://doi.org/10.1186/s13073-022-01020-2.
59. Rousham EK, Unicomb L, Islam MA. Human, animal and environmental contributors to antibiotic resistance in low-resource settings: integrating behavioural, epidemiological and One Health approaches. Proc Biol Sci. 2018;285:20180332. https://doi.org/10.1098/rspb.2018.0332.
60. Arnold KE, Laing G, McMahon BJ, Fanning S, Stekel DJ, Pahl O, et al. The need for One Health systems-thinking approaches to understand multiscale dissemination of antimicrobial resistance. Lancet Planet Health. 2024;8. https://doi.org/10.1016/S2542-5196(23)00278-4.

Publisher's Note